This document is a preprint of: D. Swist, A. Kumar and G. Fettweis, "Upper Bound on Side Lobe Levels for mMIMO Antennas to Evaluate the Beam Steering Capability," in IEEE Communications Letters, vol. 25, no. 1, pp. 289-293, Jan 2021. DOI:10.1109/LCOMM.2020.3025368

Upper Bound on Side Lobe Levels for mMIMO Antennas to Evaluate the Beam Steering Capability

Daniel Swist, Atul Kumar, and Gerhard Fettweis, *Fellow*, *IEEE*

***Abstract*—A promising concept to meet the growing requirements of future wireless systems is the use of massive multiple-input-multiple-output (mMIMO) systems. Specifically, in an attempt to mitigate the high cost due to the complexity of these systems, sub-array based antenna architectures are highly anticipated, where not every antenna element is independently controllable, but groups of elements are connected. Consequently, sharing the steering circuitry reduces degrees of freedom in the design of effective beam patterns. Due to this, sub-array based antenna systems suffer from severely increased side lobe levels (SLLs), which limit the steering capability of mMIMO systems. Therefore, it is difficult to establish a distinct general optimum tool for beam pattern design. Therefore, in this paper, we explore theoretically a mechanism to describe SLLs due to beam steering in uniform sub-array based mMIMO systems, and describe an analytical upper bound on the SLL distance as a function of the steering angle. The derived expression can be used to evaluate the steering capabilities of sub-array based configuration.**

***Index Terms*—Massive MIMO; beamforming; phased array; side lobe level; grating lobe; steering capability; sub-array.**

I. Introduction

The increasing data traffic demand drives adoption of massive multiple-input-multiple-output (mMIMO) technologies for enhanced communications performance through improved spectral efficiency and spatial reuse [1]. Two dimensional (2D) active antenna array (AAA) designs are a promising solution together with millimeter wave technologies [2], where high versatility steering antennas are required. However, an increasing amount of antenna elements causes a significant rise in complexity for channel estimation and the amount of required hardware, such as RF-converters, power amplifiers, and phase shifters [3].

In order to reduce the complexity and costs, an approach for certain application scenarios is sharing hardware components between individual antenna elements [4]–[6]. Therefore, more than one antenna elements are stacked together into groups to form sub-arrays. These groups receive the same amplitude and phase excitation throughout the whole sub-array groups, as opposed to full-featured mMIMO systems, where every antenna element is independently controllable [7]–[9].

The performance of mMIMO systems based on AAAs in multi-user scenarios is limited by side lobe levels (SLLs) causing interference among users. To maximize throughput, it is therefore necessary to reduce the SLLs. However, the sub-array antenna architecture inherently suffers from huge SLLs while steering and has been studied by several authors in the literature [10]–[12]. To reduce SLLs several optimization techniques have been studied using additional hardware such as lenses [13] and horn antennas [14]. Further approaches are irregular sub-array groups [15], overlapped sub-arrays [10] and displacement of antenna elements [16], which also require more complex hardware and array geometry design.

In [17], it is stated that the characterization of steering capability is in general a complex task due to the numerous parameters involved. Hence, they propose a figure of merit for comparing steering performance of antennas. However, SLLs are not taken into account. Since SLLs cause interference in mMIMO beam forming systems—ultimately limiting achievable data rates, it is necessary to consider SLLs in the analysis of steering capability when characterizing antennas with regard to overall communication system performance.

Further, given the constraint of uniform sub-arrays with the amplitude and phase excitation weights, as well as the antenna element distances being the control parameters, no explicit limit on the steering range for a desired maximum SLL has been stated. In the process of pattern optimization it is therefore vital to express the possible extent of steering capability improvement in terms of side lobes in general without dependence on the weights themselves.

Therefore, we explore the SLLs due to the grating lobes in uniform sub-arrays in beam steering scenarios theoretically, and a general upper bound on the SLL distance as a function of the steering angle is derived analytically. This allows to determine the steering capability for a given sub-array configuration. Moreover, we also confirm the derived results through different optimization techniques by means of simulation.

II. Mathematical Modeling

A right-handed coordinate system is assumed with axes x, y and z. The considered system is a planar rectangular antenna array, with N_r elements row-wise and N_c elements column-wise. The antenna elements are uniformly spaced in each, rows and columns, with a spacing of d_r along the x-axis and d_c along the y-axis respectively. The surface normal to the antenna plane is parallel to the z-axis. Without loss of generality, every N_{sub} elements are grouped within the rows to form a sub-array receiving the same weight excitation. The beam pattern is denoted as $F(\Theta, \Phi)$, where Θ is the angle counted from the z-axis in the xz-plane, whereas Φ is counted from the z-axis in yz-plane. For convenience, the angles Θ and Φ are referred to as azimuth and elevation angles respectively, assuming the y-axis is perpendicular w.r.t to earth surface.

The far-field azimuth pattern $F(\Theta)$=$F(\Theta, \Phi = 0)$ of N_r isotropic antenna elements within rows can be expressed for signals of a wave length λ and a wave number $k = 2\pi/\lambda$ as

$$F(\Theta) = \sum_{n=1}^{N_r} w_n s_n e^{j(knd_r \sin\Theta)} = \sum_{n=1}^{N_r} w_n s_n e^{j(k_x n d_r)} \quad (1)$$

The authors are affiliated with Vodafone Chair Mobile Communications Systems, Department of Electrical Engineering, Technische Universitat Dresden, Germany. (e-mail: daniel.swist@mailbox.tu-dresden.de; {atul.kumar, gerhard.fettweis}@tu-dresden.de)

where $k_x = k\sin(\Theta)$ is the wave vector component coinciding with the axis on which the antenna elements are located, w_n is the weight of the nth antenna element, $s_n = e^{-j(knd_r \sin\Theta_s)}$ is the steering vector with the steering angle Θ_s, and $n \cdot d_r$ is the relative distance of the elements. For the sub-array configuration, (1) can be rewritten as a product of sums

$$F(\Theta)=\underbrace{\sum_{m=1}^{N_{\text{main}}} w_m s_m e^{j(k_x(md_r N_{\text{sub}}))}}_{F_{\text{main}}(\Theta,\Theta_s)} \underbrace{\sum_{l=1}^{N_{\text{sub}}} e^{j(k_x(ld_r))}}_{F_{\text{sub}}(\Theta)} \tag{2}$$

where $N_{\text{main}} = N_r/N_{\text{sub}}$ is the amount of sub-array antenna groups and w_m is the complex-valued weight for the mth sub-array. As can be seen in (2), the pattern of the sub-array is completely independent of the pattern of the main array. This implies that adjusting weights or steering only controls the main array pattern while the sub-array pattern stays fixed. Since the antenna elements within each sub-array group share the same weight, the normalized magnitude of the sub-array pattern can be written as

$$|F_{\text{sub}}(\Theta)| = \left| \frac{1}{N_{\text{sub}}} \frac{\sin(\frac{N_{\text{sub}}}{2} k_x d_r)}{\sin(\frac{1}{2} k_x d_r)} \right| \tag{3}$$

A. Zeros in Sub-Array Pattern

From (3) it is obvious that the sub-array pattern is zero for specific angles Θ. Since the sub-array pattern does not depend on the weights nor on the steering vector, the pattern will not change when steering is applied. Therefore, the angle $\Theta{=}\Theta_{\text{zero}}$ of the zero closest to center can be determined from (3) as $\Theta_{\text{zero}} = \pm\sin^{-1}\left(\frac{2\pi}{kd_r N_{\text{sub}}}\right)$. Consequently, the positions of the zeros depend on the choice of parameters d_r, N_{sub} for a given wavelength $\lambda = 2\pi/k$. Steering towards these angles will result in partial cancellation of the main beam.

B. Grating Lobes of Main Array Pattern

The main array pattern in (2) is affected by an effectively extended antenna spacing $d_{\text{main}}{=}d_r{\cdot}N_{\text{sub}}$ instead of the actual physical spacing d_r of the individual elements. This may cause grating lobes in the visible range, which appear a period of $2\pi/d_{\text{main}}$ away from the main beam center in wave vector domain. Without steering, the grating lobes appear symmetrically around the center $k\sin\Theta{=}0$, and the center points of the grating lobes are located at $\Theta{=}\sin^{-1}\left(\pm\frac{2\pi}{kd_{\text{main}}}\right){=}\pm\sin^{-1}\left(\frac{2\pi}{kd_r N_{\text{sub}}}\right)$, which is the exact same position as the zeros of the sub-array pattern. Therefore, grating lobes are maximally cancelled out.

When steering the main beam, the grating lobes are shifted as well and move out of the multiplicative nulling-region of the sub-array pattern, thus increasing in level, and effectively limiting the maximum extent of achievable grating lobe suppression. Consequently, there is a steering angle at which the main beam and a grating lobe will have the same level. Assuming a symmetric main beam, this specific steering angle $\Theta_s = \Theta_{\text{equal}}$ corresponds to a shift of half the main beam pattern period in wave vector domain π/d_{main}, and can then be written as $\Theta_{\text{equal}} = \sin^{-1}\left(\pm\frac{\pi}{kd_{\text{main}}}\right) = \pm\sin^{-1}\left(\frac{\pi}{kd_r N_{\text{sub}}}\right)$. Since the sub-array pattern in (3) has a main lobe at the center

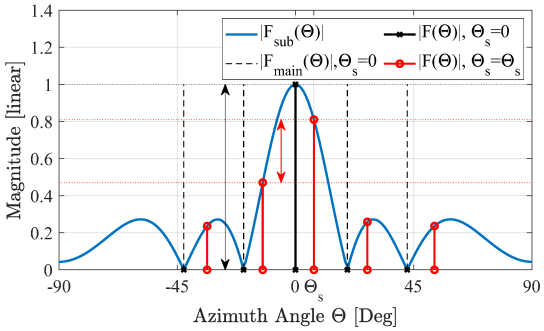

Fig. 1: Patterns of sub-array F_{sub}, main array F_{main} (N_{sub}=4, d_r=0.74λ), and resulting pattern F for narrow beam with and without steering, where the red and black arrows indicate the peak SLL distances respectively.

dominating in level, the grating lobes closest to the center will constitute the highest side lobe levels when steering, so analysis of the first zeros is sufficient.

III. Modeling of Upper Bound on Side Lobe Level

Modeling of an upper bound on the SLL distance throughout the steering range is performed by analyzing two ideal cases analytically: narrow beam and rectangular beam. For that, the relative SLL distance is defined as the magnitude ratio of the peak main beam level $F(\Theta_{\text{ML}})$ and the peak level of the side lobe $F(\Theta_{\text{SL}})$: $SLL = \left|\frac{F(\Theta_{\text{ML}})}{F(\Theta_{\text{SL}})}\right|$

A. Narrow Beam

First, we consider an idealized main beam pattern F_{main} with zero beam width as simple approximation of a narrow pencil beam commonly encountered in millimeter-wave applications. The magnitude is 1 at $\Theta = 0$ and 0 elsewhere within one period. The angle of the main beam peak Θ_{ML} when steering towards Θ_s is then $\Theta_{\text{ML}} = \Theta_s$. Consequently, the dominating grating lobe image will appear a period of $2\pi/d_{\text{main}} = 2\pi/(d_r N_{\text{sub}})$ apart from the main beam in wave vector domain, and can be written in angular domain as

$$\Theta_{\text{SL}} = \sin^{-1}\left(\sin\Theta_s - \frac{2\pi}{kd_r N_{\text{sub}}}\right) \tag{4}$$

Fig. 1 shows a principle illustration of the narrow beam consideration, where the increase in magnitude of the first grating lobe due to steering is visible. The reduced SLL distance while steering is indicated by the red arrow, compared to the case of no steering indicated by the black arrow, where the grating lobes are completely cancelled out. Using the SLL definition and (3) the SLL distance for the narrow beam case can be written as a function of the steering angle Θ_s

$$SLL_{\text{nrw}}(\Theta_s) = \left| \frac{\sin\left(\frac{\pi}{N_{\text{sub}}} - \frac{d_r}{2} k\sin\Theta_s\right)}{\sin\left(\frac{d_r}{2} k\sin\Theta_s\right)} \right| \tag{5}$$

Fig. 2 shows a plot of the SLL distance of the narrow beam case for different N_{sub}. However, this approaches infinity towards values of Θ close to zero and does not show any information about the impact of the beam width of a beam. For valid results, the zeros and grating lobes need to lie inside the visible range. The condition is $\frac{\lambda}{d_r N_{\text{sub}}} < 1$, which constitutes a minimal d_r for given λ and N_{sub}.

This document is a preprint of: D. Swist, A. Kumar and G. Fettweis, "Upper Bound on Side Lobe Levels for mMIMO Antennas to Evaluate the Beam Steering Capability," in IEEE Communications Letters, vol. 25, no. 1, pp. 289-293, Jan 2021. DOI:10.1109/LCOMM.2020.3025368

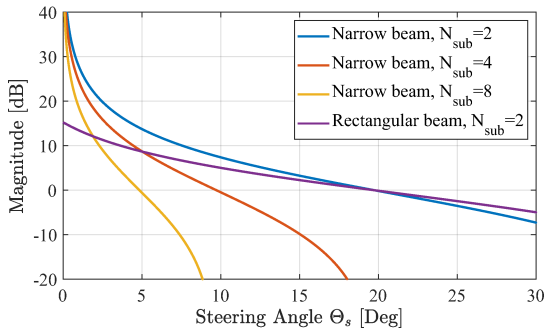

Fig. 2: Side lobe level distance as function of steering angle for narrow beam and rectangular beam ($\Theta_{\text{BW}} = 8.571°$), $d_r = 0.74\lambda$

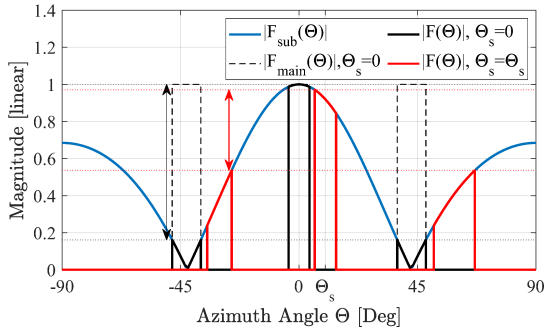

Fig. 3: Patterns of sub-array F_{sub}, main array F_{main} (N_{sub}=2, d_r=0.74λ), and resulting pattern F for rectangular beam with and without steering, where the red and black arrows indicate the peak SLL distances respectively.

B. Rectangular Beam

To model the impact of beam width on SLLs, an ideal rectangular main beam pattern F_{main} is assumed here, with a level of 1 for $|\Theta| \leq \Theta_{\text{BW}}/2$ and a magnitude of 0 elsewhere within one period. Θ_{BW} is the beam width in angular domain when no steering is applied. Fig. 3 shows the reduced SLL distance while steering indicated by the red arrow, compared to the no-steering case indicated by the black arrow. Note there are non-zero SLLs even without steering.

As opposed to the narrow consideration, the peak level of the main beam will not always appear at the nominal steering angle Θ_s. The peak level of the main beam will stay at $\Theta = 0$ for steering angles $\Theta_s \leq \Theta_{\text{BW}}/2$ due to the nature of the rectangular function. For steering angles $\Theta_s > \Theta_{\text{BW}}/2$ the main beam peak level will appear at the edge of the main beam nearest to the center. The angle Θ_{ML} of the main beam peak level can thus be expressed as a section-wise defined function:

$$\Theta_{\text{ML}} = \begin{cases} 0, & \Theta_s \leq \frac{1}{2}\Theta_{\text{BW}} \\ \sin^{-1}\left(\sin\Theta_s - \sin\frac{1}{2}\Theta_{\text{BW}}\right), & \Theta_s > \frac{1}{2}\Theta_{\text{BW}} \end{cases} \quad (6)$$

The grating lobe maximum peak appears at the edge of the grating lobe closer to the center and the position can be expressed as

$$\Theta_{\text{SL}} = \sin^{-1}\left(\sin\Theta_s - \frac{2\pi}{kd_r N_{\text{sub}}} + \sin\frac{1}{2}\Theta_{\text{BW}}\right) \quad (7)$$

Using (3) together with (6) and (7) the SLL distance for the rectangular beam can be expressed as

$$SLL_{\text{rct}}(\Theta_s) = \begin{cases} \left|\frac{\sin(a^+ - \frac{\pi}{N_{\text{sub}}})}{\sin(N_{\text{sub}}a^+)} \; \frac{\sin(N_{\text{sub}}a^-)}{\sin(a^-)}\right|, & \Theta_s > \frac{1}{2}\Theta_{\text{BW}} \\ \left|\frac{\sin(a^+ - \frac{\pi}{N_{\text{sub}}})}{\frac{1}{N_{\text{sub}}}\sin(N_{\text{sub}}a^+)}\right|, & \Theta_s \leq \frac{1}{2}\Theta_{\text{BW}} \end{cases} \quad (8)$$

where $a^+ = \frac{kd_r}{2}(\sin\Theta_s + \sin\frac{1}{2}\Theta_{\text{BW}})$, $a^- = \frac{kd_r}{2}(\sin\Theta_s - \sin\frac{1}{2}\Theta_{\text{BW}})$. The center-facing border of the dominating rectangular grating lobe must be within the visible range, and the condition is $\frac{\lambda}{d_r N_{\text{sub}}} - \sin(\frac{1}{2}\Theta_{\text{BW}}) < 1$. This implies a minimal d_r depending on the parameters λ, N_{sub} and Θ_{BW}. Note that while being an idealized consideration, an angular deviation between the maximum peak angle of the main beam and the nominal steering angle will be present for any practical beam to some extent as well. Fig. 2 shows the SLL distance for the rectangular beam compared to the narrow case. As expected, even without steering the SLL distance is severely limited.

C. An Upper Bound for Side Lobe Levels

From the considerations of sections III-A and III-B an upper bound on the SLL distance throughout the steering range can be determined when certain assumptions about the main beam specification are made:

- main beam is symmetric around center $\Theta = 0$
- main beam has a peak at center $\Theta = 0$
- main beam has a half power beam width of Θ_{3dB}

Note this also inherently implies that the main beam can have arbitrary levels ≤ 1 within a rectangular mask confined by the half power beam width Θ_{3dB}.

Although derived from the narrow beam assumptions, the narrow beam SLL distance in (5) is also an upper bound on main beams fitting the mentioned assumptions above. The magnitude of the sub-array beam pattern $F_{\text{sub}}(k_x)$ is monotonically decreasing away from the center $\Theta = 0$ towards $\Theta = \Theta_{\text{zero}}$ with respect to $k_x = k\sin\Theta$. This implies that the main lobe narrow level $F_{\text{ML}}(\Theta_s)$ is greater or equal than the grating lobe narrow level $F_{\text{SL}}(\Theta_s)$ for $0 \leq \Theta_s \leq |\Theta_{\text{equal}}|$:

$$F_{\text{ML}}(\Theta_s) = F_{\text{sub}}(k_x) \geq F_{\text{sub}}(k_x - \frac{2\pi}{d_r N_{\text{sub}}}) = F_{\text{SL}}(\Theta_s) \quad (9)$$

where $k_x = k\sin\Theta_s$. As the main beam is assumed symmetric, any point within the rectangular mask of the main beam $F'_{\text{ML}}(\Theta_s) = a \cdot F_{\text{sub}}(k(\sin\Theta_s - \sin\Theta'))$ with level $a \leq 1$ and distance from the narrow center image $\sin\Theta' \leq \sin\Theta_{\text{3dB}}/2$ appears as a grating lobe image $F'_{\text{SL}}(\Theta_s) = a \cdot F_{\text{sub}}(k(\sin\Theta_s + \sin\Theta') - 2\pi/d_{\text{main}})$. The sub-array beam pattern $F_{\text{sub}}(k\sin\Theta)$ in wave vector representation has a negative curvature in the range of $0 \leq |k\sin\Theta| \leq |k\sin\Theta_{\text{equal}}| = \pi/d_{\text{main}}$ and the absolute value of the slope of the sub-array beam pattern for $0 \leq |k\sin\Theta| \leq |k\sin\Theta_{\text{equal}}|$ is less than in the range $|k\sin\Theta_{\text{equal}}| \leq |k\sin\Theta| \leq |k\sin\Theta_{\text{zero}}|$. Since steering causes a linear shift of the main beam pattern in wave vector domain (i.e. same shift for main beam and grating lobe), any level deviation of the main beam $\Delta F_{\text{ML}}(\Theta_s) = F'_{\text{ML}}(\Theta_s) - F_{\text{ML}}(\Theta_s) > 0$ is less than or equal to the corresponding level deviation of the grating lobe $\Delta F_{\text{SL}}(\Theta_s)$ expressed as

$$\Delta F_{\text{SL}}(\Theta_s) = F'_{\text{SL}}(\Theta_s) - F_{\text{SL}}(\Theta_s) \geq \Delta F_{\text{ML}} \quad (10)$$

From (9) and (10) follows:

$$\frac{\Delta F_{\text{SL}}(\Theta_s)}{F_{\text{SL}}(\Theta_s)} \geq \frac{\Delta F_{\text{ML}}(\Theta_s)}{F_{\text{ML}}(\Theta_s)}, \quad 0 \leq \Theta_s \leq |\Theta_{\text{equal}}| \quad (11)$$

and thus:

This document is a preprint of: D. Swist, A. Kumar and G. Fettweis, "Upper Bound on Side Lobe Levels for mMIMO Antennas to Evaluate the Beam Steering Capability," in IEEE Communications Letters, vol. 25, no. 1, pp. 289-293, Jan 2021. DOI:10.1109/LCOMM.2020.3025368

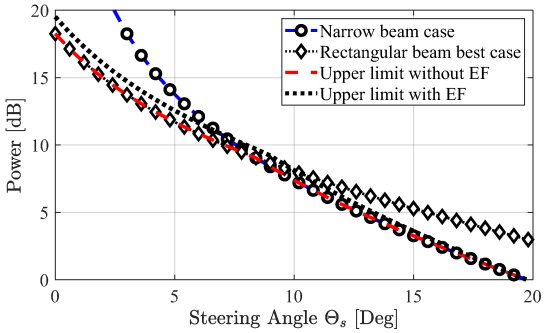

Fig. 4: Upper bound on side lobe level distance throughout steering range for $N_{\text{sub}} = 2$, $\Theta_{\text{BW}} = 8.571°$

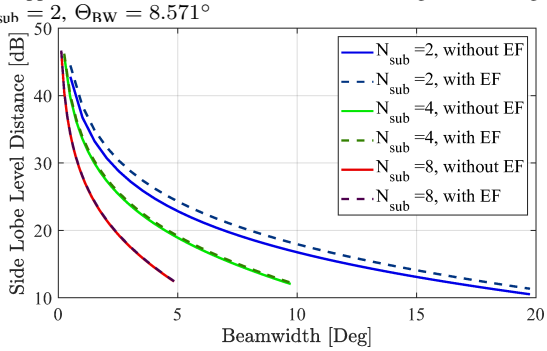

Fig. 5: Upper bound on side lobe level distance as function of beam width at zero steering ($\Theta_s = 0$)

$$\frac{F_{\text{ML}}(\Theta_s)}{F_{\text{SL}}(\Theta_s)} = SLL_{\text{nrw}} \geq \frac{F'_{\text{ML}}(\Theta_s)}{F'_{\text{SL}}(\Theta_s)} \tag{12}$$

Hence, the narrow beam SLL distance cannot be surpassed by any beam meeting the specifications, and poses an upper bound. From the rectangular beam consideration in section III-B a best case scenario can be derived, which also poses an upper bound:

- best assumable case for main beam level: as the beam is assumed to have levels ≤ 1 within a rectangular mask with width of Θ_{3dB}, the best possible case is the main beam level as in the rectangular case in section III-B.
- best assumable case for SLL: the lowest possible generally assumable beam level of the grating lobe appears at the images of the half power points with a level of $1/2$.

The SLL at the half power points of the grating lobe can be expressed using the results from the rectangular case in (8) by identifying the beam width of the rectangular beam with the half power beam width $\Theta_{\text{3dB}} = \Theta_{\text{BW}}$ and multiplying by $\sqrt{2}$, then $SLL_{\text{3dB}}(\Theta_s) = \sqrt{2} \cdot SLL_{\text{rct}}(\Theta_s)$. With both considerations posing an upper bound, the minimum of both poses a total lower upper bound, closer to the achievable limit (Fig. 4). Note that the SLL distance is limited in the zero steering case $\Theta_s = 0$, and shows a strong dependence on the 3dB beam width of the main beam alone as shown in Fig. 5. When $d_r \geq (1 - \frac{1}{2N_{\text{sub}}})\lambda$, the center of a main beam grating lobe will be present in the visible range for some $\Theta_s \leq \Theta_{\text{equal}}$, which is not cancelled out by a zero since the main lobe of the sub-array pattern repeats itself within the visible range, so achievable SLLs might be lower. However, if the antenna elements have a high attenuation towards $\pm 90°$, then level deviations only become relevant for values of d_r close to 1λ.

D. Element Factor Influence

The previous results are valid for isotropic antenna elements. A realistic antenna element will not achieve such an ideal uniform pattern. The element pattern $EF(\Theta)$ can be modeled as another multiplicative component of the total resulting beam pattern [18]. Therefore, the total pattern of the antenna array F_Σ can then be written as the product of the individual patterns $F_\Sigma(\Theta) = F_{\text{main}}(\Theta) \cdot F_{\text{sub}}(\Theta) \cdot EF(\Theta)$.

For element patterns which have negative curvature in wave vector domain and are symmetric around the center $\Theta = 0$, the SLL distances as described in the previous sections can be adjusted using a corrective factor $SLL_{EF} = \left| \frac{EF(\Theta_{\text{ML}})}{EF(\Theta_{\text{SL}})} \right|$, where Θ_{ML}, Θ_{SL} are the angles $\Theta_{\text{ML}} = \Theta_s$, (4) and (6), (7) for narrow and rectangular beam case respectively. The total SLL distance can then be written as $SLL_\Sigma = SLL \cdot SLL_{EF}$. This is a general formula, which needs to be evaluated for the specific antenna parameters given by a model or obtained through measurement.

To illustrate the impact of an element response, we consider cosine elements $EF(\Theta) = \cos^m(\Theta)$ with $m = 0.65$. For the narrow case (5) using (4) the SLL distance due to the element factor can be expressed as

$$SLL_{EFn}(\Theta_s) = \frac{\cos^m(\Theta_s)}{\cos^m\left(\sin^{-1}\left(\sin\Theta_s - \frac{\lambda}{d_r N_{\text{sub}}}\right)\right)} \tag{13}$$

and for the rectangular case (8)—respectively also for the 3dB best case—using (6) and (7) as

$$SLL_{EFr}(\Theta_s) = \frac{\cos^m\left(\sin^{-1}\left(\sin\Theta_s - \frac{1}{2}\sin\Theta_{\text{3dB}}\right)\right)}{\cos^m\left(\sin^{-1}\left(\sin\Theta_s - \frac{\lambda}{d_r N_{\text{sub}}} + \frac{1}{2}\sin\Theta_{\text{3dB}}\right)\right)} \tag{14}$$

The impact of the cosine element pattern is shown in Fig. 4 and shows improved SLL performance. More sophisticated antenna models can be evaluated analogously using the presented procedure in analytical terms if $EF(\Theta)$ is explicitly given as function of Θ.

IV. Beam Pattern Optimization

Since an upper bound has been derived in general, which is not necessarily achieved for arbitrary weights w_n, several optimization approaches were performed to achieve a close match with the theoretical results regarding peak SLL. We used a Taylor window and the meta-heuristic algorithms invasive weed optimization (IWO) and particle swarm optimization (PSO). The IWO as per [19] identifies sets of weights w_n with weed that generate offspring based on their performance, and ultimately selection takes place. In [20], the used PSO is described, where sets of weights w_n are identified with particles moving in parameter space based on their performance.

The resulting beam patterns are shown in Fig. 6, including also uniform weights ($w_n = 1$) for reference. Note that the results for IWO and PSO are nearly indistinguishable, as the obtained weights are also close to linear dependency. At $\Theta_s = 0$ the dominating SLL in the uniform case is not constituted by a grating lobe, but by the minor side lobes (side lobes within on period of the main beam pattern). When a beam with the peak at the center is desired, only the minor side lobes can be reduced at the expense of increasing beam width, causing increased grating lobes due to the sub-array. In the Taylor window case, the minor side lobes are reduced. However, the peak SLL is now caused by the grating lobes,

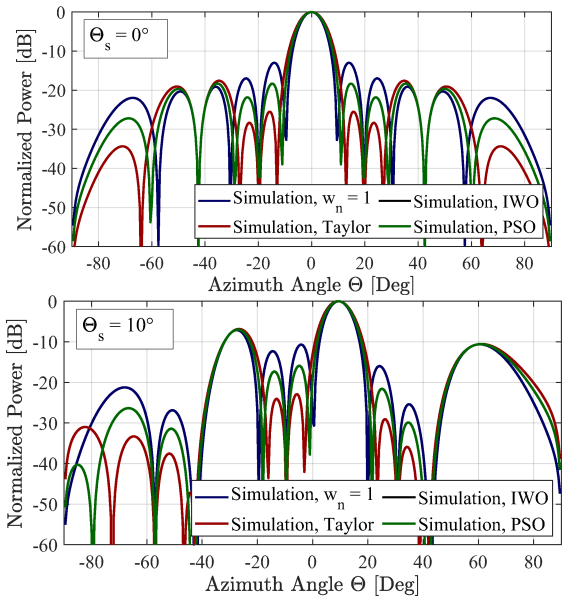

Fig. 6: Patterns of the simulated weights for different steering angles Θ_s

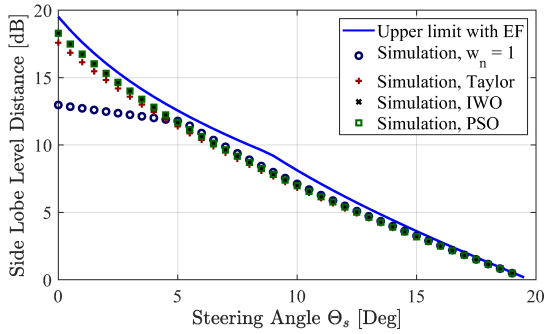

Fig. 7: Simulated results for different weights compared against upper limit for $N_{\text{sub}} = 2$ and $d_r = 0.74\lambda$

as the beam width increased due to the weight adjustment, which is now lesser cancelled out by the sub-array pattern zeros. The IWO and PSO effectively produced weights where the increase of the grating lobe level due to the reduction of minor side lobes is balanced out. This trade-off is inherently caused by susceptibility of the sub-array antenna to grating lobes. For $\Theta_s = 10°$ it is visible that the grating lobe is clearly dominating in level for all cases with only little difference.

V. Simulation Results

Simulations have been performed for all weight sets obtained using the methods in section IV and compared to the analytical results presented in III. The resulting SLL distances are shown in Fig. 7. As expected the uniform case shows a high deviation from the upper bound for lower steering angles, where optimization potential was expected. The Taylor window case shows improved performance, and the IWO and PSO show best performance close to the upper bound. While still not reaching the limit, no significant increase in SLL distance can be expected from the obtained weights that are more than 1.5 dB. It shows that the theoretical results can be a useful reference in the optimization process to get a close prediction with simple analytical tools.

VI. Conclusion

Massive MIMO systems using sub-array based steering antennas can greatly increase deployment possibilities, but they inherently suffer from the SLL while steering the antenna. Therefore, an upper bound on the SLL distance as a function of the steering angle is derived analytically, from which the steering capability can be determined for a given uniform sub-array configuration. Optimization of weights has been performed to achieve improved SLL performance, and a close match to the derived results was confirmed by simulation. Hence, the presented analytical framework is a useful reference in the optimization process, and also allows assessing a steering capability in terms of SLLs that can be used in the analysis of interference in mMIMO systems. The results also show that no significant improvement can be expected optimizing the antenna weights on a per-sub-array-group level alone.

References

[1] F. Rusek *et al.*, "Scaling up mimo: Opportunities and challenges with very large arrays," *IEEE Signal Processing Magazine*, vol. 30, Jan. 2012.
[2] S. Ghosh and D. Sen, "An inclusive survey on array antenna design for millimeter-wave communications," *IEEE Access*, vol. 7, pp. 83137–83161, Jun. 2019.
[3] T. L. Marzetta *et al.*, *Fundamentals of Massive MIMO*. Cambridge University Press, 2016.
[4] I. Ahmed *et al.*, "A survey on hybrid beamforming techniques in 5g: Architecture and system model perspectives," *IEEE Communications Surveys Tutorials*, vol. 20, pp. 3060–3097, Jun. 2018.
[5] Y. Zou, W. Rave, and G. Fettweis, "Analog beamsteering for flexible hybrid beamforming design in mmwave communications," in *European Conference on Networks and Communications*, pp. 94–99, Jun. 2016.
[6] M. Shehata *et al.*, "On the theoretical limits of beam steering in mmwave massive mimo channels," in *IEEE 30th Annual International Symposium on PIMRC*, pp. 1–6, Sep. 2019.
[7] Y. Gao and T. Kaiser, "Antenna selection in massive mimo systems: Full-array selection or subarray selection?," in *IEEE SAM Workshop*, pp. 1–5, Jul. 2016.
[8] X. Song, W. Rave, N. Babu, S. Majhi, and G. Fettweis, "Two-level spatial multiplexing using hybrid beamforming for millimeter-wave backhaul," *IEEE Transactions on Wireless Communications*, vol. 17, pp. 4830–4844, May 2018.
[9] A. Kumar, J. Bartelt, A. N. Barreto, and G. Fettweis, "2D active antenna array design for mmimo to improve spectral and energy efficiency," in *2nd IEEE 5G World Forum (5GWF)*, pp. 490–495, Sep. 2019.
[10] R. J. Mailloux, *Electronically Scanned Arrays*, vol. 2. Morgan Claypool, Jan. 2007.
[11] R. J. Mailloux, *Phased Array Antenna Handbook*. USA: Artech House, Inc., 3rd ed., 2017.
[12] A. Bhattacharyya, *Phased Array Antennas: Floquet Analysis, Synthesis, BFNs and Active Array Systems*. Wiley Series in Microwave and Optical Engineering, Wiley, 2006.
[13] R. J. Mailloux, "Subarray technology for large scanning arrays," in *The Second European Conference on Antennas and Propagation, EuCAP 2007*, pp. 1–6, Nov. 2007.
[14] R. Mailloux and G. Forbes, "An array technique with grating-lobe suppression for limited-scan applications," *IEEE Transactions on Antennas and Propagation*, vol. 21, pp. 597–602, Sep. 1973.
[15] H. Wang, D.-G. Fang, and Y. Chow, "Grating lobe reduction in a phased array of limited scanning," *Antennas and Propagation, IEEE Transactions on*, vol. 56, pp. 1581 – 1586, Jul. 2008.
[16] A. P. Goffer, M. Kam, and P. R. Herczfeld, "Design of phased arrays in terms of random subarrays," *IEEE Transactions on Antennas and Propagation*, vol. 42, pp. 820–826, Jun. 1994.
[17] J. G. Marin *et al.*, "Figure of merit for beam-steering antennas," in *12th German Microwave Conference (GeMiC)*, pp. 44–47, Mar. 2019.
[18] C. Balanis, *Antenna Theory: Analysis and Design*. Wiley, 2012.
[19] S. Pal *et al.*, "Linear antenna array synthesis with invasive weed optimization algorithm," in *2009 International Conference of Soft Computing and Pattern Recognition*, pp. 161–166, Dec. 2009.
[20] Y.-D. Zhang, S. Wang, and G. Ji, "A comprehensive survey on particle swarm optimization algorithm and its applications," *Mathematical Problems in Engineering*, vol. 2015, pp. 1–38, Jan. 2015.